

$$\left. \begin{aligned} \partial\psi_0(\mathbf{r})/\partial s_0 &= -i\pi K\chi_{\bar{h}}(\mathbf{r})\psi_h(\mathbf{r}), \\ \partial\psi_h(\mathbf{r})/\partial s_h &= -i\pi K\chi_h(\mathbf{r})\psi_0(\mathbf{r}) + i2\pi K\beta_h\psi_h(\mathbf{r}) \end{aligned} \right\} \quad (8)$$

which hold also for X-rays, if $\chi_h(\mathbf{r})$ is read as the Fourier coefficient of 4π times the polarizability of the crystal with appropriate polarization factor. The boundary conditions at the entrance surface are expressed in similar form as in the ordinary theory, namely

$$\left. \begin{aligned} \psi_0(\mathbf{r}_e) &= \Psi_0(\mathbf{r}_e) \\ \psi_h(\mathbf{r}_e) &= 0 \end{aligned} \right\} \quad (9)$$

where \mathbf{r}_e is a position vector on the entrance surface, and $\Psi_0(\mathbf{r}_e)$ the amplitude of the incident wave in vacuum. The fact that both sides of (9) are slowly varying functions of position instead of constants is important; incident waves other than plane waves can be treated as well. One of the methods of solution of (8) is to convert

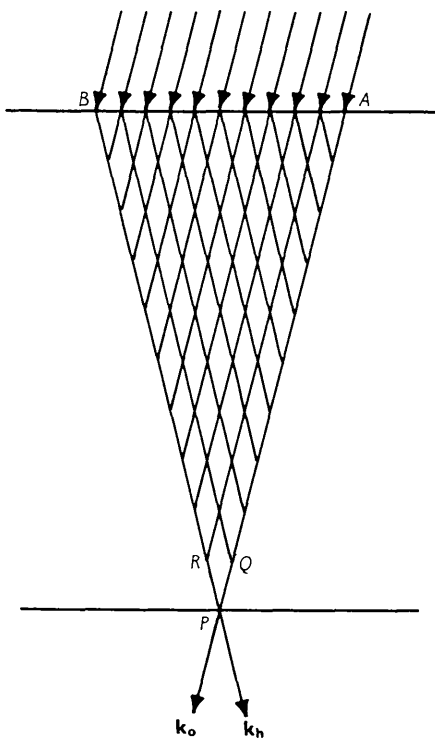


Fig. 1. Schematic drawing showing methods of solution of equation (8). The upper arrows and one of the lower ones are in the direction of the incident wave or of \mathbf{k}_o , and the other lower one in that of \mathbf{k}_h . The solutions at P on the exit surface are determined by the part of the incident wave falling between A and B , and can be calculated either by the method of Riemann functions or by successive numerical calculations at each mesh point.

it into second-order partial differential equations for ψ_0 and ψ_h , each of which have a hyperbolic form which is capable of solution by the method of Riemann functions. This method gives the solution at a point P inside or on the exit surface of the crystal by a surface integral over AB (Fig. 1) where A and B are points on the entrance surface such that AP and BP are, respectively, parallel to \mathbf{k}_o and \mathbf{k}_h . The integral involves $\Psi_0(\mathbf{r}_e)$ and the Riemann function for this particular point P given by the values of χ_h , $\chi_{\bar{h}}$ and β_h inside the triangle PAB , and its derivatives. This result is of theoretical importance, since it shows that only values of the amplitude of the incident wave falling between A and B contribute to the wave function at P , providing a theoretical basis for the column approximation in the electron case where the triangle PAB reduces to a thin column owing to the small Bragg angle. Equation (8) is also capable of a numerical solution. It includes only the derivatives $\partial\psi_0/\partial s_0$ and $\partial\psi_h/\partial s_h$ out of four possible first-order ones. This shows that if we divide the triangle PAB by a fine mesh with axes parallel to \mathbf{k}_o and \mathbf{k}_h , as shown in Fig. 1, the value of ψ_0 at P , say, is determined by the values of ψ_0 and ψ_h at Q , and that of ψ_h at P , by those of ψ_0 and ψ_h at R and so on. The repetition of this process from the top surface AB to the bottom will give the solution at P .

The author would like to express his sincere thanks to Dr A. R. Lang for his encouragement and advice, and to Prof. M. H. L. Pryce, Prof. F. C. Frank and Dr M. E. Foglio for their suggestions and discussions. Financial support from the European Office, Office of Aerospace Research, USAF, is gratefully acknowledged.

References

- COWLEY, J. M. & MOODIE, A. F. (1957). *Acta Cryst.* **10**, 609.
 EWALD, P. P. (1933). *Handbuch der Physik*, **23**, 2, p. 290. Berlin: Springer.
 HIRSCH, P. B., HOWIE, A. & WHELAN, M. J. (1960). *Phil. Trans. Roy. Soc. A*, **252**, 499.
 HOWIE, A. & WHELAN, M. J. (1960). *Proc. Eur. Reg. Conf. on Electron Microscopy, Delft*, Vol. 1, p. 194.
 HOWIE, A. & WHELAN, M. J. (1961). *Proc. Roy. Soc. A*, **263**, 217.
 HOWIE, A. & WHELAN, M. J. (1962). *Proc. Roy. Soc. A*, **267**, 206.
 KATO, N. & LANG, A. R. (1959). *Acta Cryst.* **12**, 787.
 KATO, N. (1960). *Acta Cryst.* **13**, 1091.
 KATO, N. (1962). (To be published.)
 LAUE, M. VON (1960). *Röntgenstrahlinterferenzen*, p. 337. Frankfurt am Main: Akademische Verlagsgesellschaft.
 STURKEY, L. (1960). Private communication.

Acta Cryst. (1962). **15**, 1312

Epitaxial growth of rutile on oxidation of titanium carbide. By K. H. G. ASHBEE and W. T. EELES, Central Electricity Generating Board, Berkeley Nuclear Laboratories, Gloucestershire, England

(Received 19 July 1962)

Thin films of the rutile modification of titanium dioxide have been grown by Ashbee & Smallman (1962) on the

(100) surfaces of TiC single crystals by oxidation in air at pressures $\sim 10^{-3}$ cm. in the temperature range 800

to 1000 °C. TiC is face-centred cubic with $a=4.32$ Å, and rutile is body-centred tetragonal with $a=4.59$, $c=2.96$ Å. The present note reports the identification of the orientation relationship between the oxide film and the parent carbide crystal.

The orientation of a flake of rutile which had been cleaved from the TiC crystal was determined by taking a series of X-ray oscillation photographs. From these photographs it was evident that the oxide grows with

its (110) plane parallel to the (100) TiC surface. Each photograph showed reflections from two (110) rutile films which are orthogonally inclined about the [110] axis.

To find the complete orientation relationship, a TiC crystal having its oxide surface layer intact was examined by taking glancing-incidence oscillation photographs, the axis of oscillation being parallel to a cube axis. It was found that the rutile tetrad axis is parallel to one of the TiC cube axes lying in the surface of the crystal so that the complete orientation relationship is

$$(100) \text{TiC} \parallel (110) \text{TiO}_2 \text{ with } [010] \text{TiC} \parallel [001] \text{TiO}_2.$$

As before, two strong rutile patterns were obtained simultaneously, corresponding to the two possible orientations of the tetrad axis given above.

Comparison of the lattice vectors (x) which define the above orientation relationship shows that

$$x[010]\text{TiC}/x[001]\text{TiO}_2 = 1.46 \text{ and} \\ x[001]\text{TiC}/x[\bar{1}10]\text{TiO}_2 = 0.667$$

which means that, at the carbide-oxide interface, three $x[010]\text{TiC}$ vectors fit two $x[001]\text{TiO}_2$ vectors with a misfit of only 2.74% and that two $x[001]\text{TiC}$ vectors match three $x[\bar{1}10]\text{TiO}_2$ vectors with no misfit. Consequently, we postulate an oxidation mechanism based on Fig. 1. This involves only small lateral translations. During oxidation there is no requirement for titanium atoms to diffuse outwards normally to the parent TiC (100) surface but as each successive sheet of Ti atoms reacts there must be an overall uniform movement of the rutile film along the [100] TiC direction to allow for the difference in specific volume.

We are indebted to the Director of Berkeley Nuclear Laboratories for permission to publish this work.

Reference

ASHBEE, K. H. G. & SMALLMAN, R. E. (1962). *Phil. Mag.* (In press.)

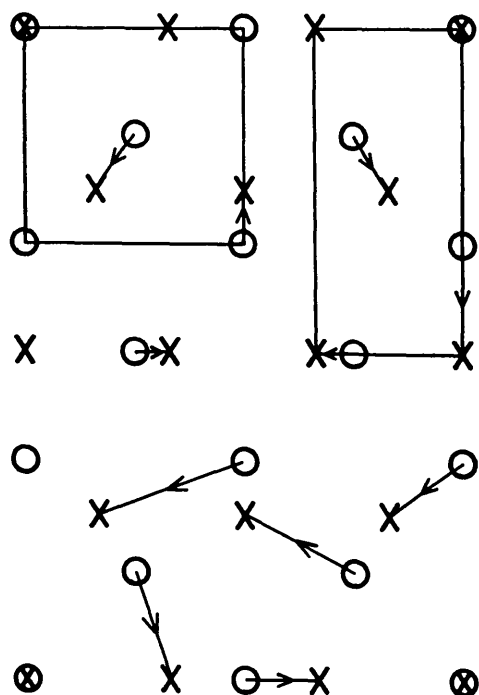


Fig. 1. Titanium atomic positions at the carbide-oxide interface. Positions in TiC are denoted ○, positions in TiO₂ ×. The arrows indicate one possible set of small lateral movements of Ti atoms which would be involved in the oxidation of this plane of TiC to TiO₂.

Acta Cryst. (1962). **15**, 1313

The unit-cell dimensions of silver azide. By H. E. MARR, III and R. H. STANFORD, JR., *Gates and Crellin Laboratories of Chemistry,* California Institute of Technology, Pasadena, California, U. S. A.*

(Received 29 June 1962)

Crystallographic studies of silver azide, AgN₃, have been made by Bassiere (1935), West (1936), Hughes (1935), Pfeiffer (1949), and Dewing, Hughes, & Pfeiffer (1962). It crystallizes in the orthorhombic space group *Ibam* and the unit cell dimensions given by previous investigators are:

	a_0	b_0	c_0
Bassiere	5.59 Å	5.94 Å	6.05 Å
West	5.59	5.91	5.97
Hughes	5.66	5.94	5.99
Dewing <i>et al.</i>	5.60	5.92	6.00

* Contribution No. 2870 from the Gates and Crellin Laboratories of Chemistry.

The structure has been accurately determined (Dewing, Hughes, & Pfeiffer, 1962); but accurate cell dimensions and, hence, accurate bond lengths have been lacking. The determination of these dimensions was undertaken as an undergraduate research project.

The powder sample was prepared by mixing equimolar solutions of silver nitrate and sodium azide and allowing the precipitate to form in the dark over night. Two powder photographs were taken with a Straumanis-type camera with a nominal radius of 9.9662 cm. using Cu $K\alpha$ radiation. Potassium chloride lines were superimposed on one of the photographs to provide a check.

The α_1 and α_2 doublets of three high angle reflections which could be unambiguously indexed were measured